The EMBO Journal (2007) 26, 3157–3168 | © 2007 European Molecular Biology Organization | All Rights Reserved 0261-4189/07
www.embojournal.org

THE EMBO JOURNAL

Interaction of HapX with the CCAAT-binding complex—a novel mechanism of gene regulation by iron

Peter Hortschansky[1,5], Martin Eisendle[2,5], Qusai Al-Abdallah[1], André D Schmidt[1], Sebastian Bergmann[1], Marcel Thön[1], Olaf Kniemeyer[1], Beate Abt[2], Birgit Seeber[2], Ernst R Werner[3], Masashi Kato[4], Axel A Brakhage[1,*] and Hubertus Haas[2,*]

[1]Department of Molecular and Applied Microbiology, Leibniz Institute for Natural Product Research and Infection Biology (HKI), and Friedrich-Schiller-University Jena, Jena, Germany, [2]Division of Molecular Biology, Biocenter, Innsbruck Medical University, Innsbruck, Austria, [3]Division of Biological Chemistry, Biocenter, Innsbruck Medical University, Innsbruck, Austria and [4]Department of Biological Mechanisms and Functions, Graduate School of Bioagricultural Sciences, Nagoya University, Nagoya, Japan

Iron homeostasis requires subtle control systems, as iron is both essential and toxic. In *Aspergillus nidulans*, iron represses iron acquisition via the GATA factor SreA, and induces iron-dependent pathways at the transcriptional level, by a so far unknown mechanism. Here, we demonstrate that iron-dependent pathways (e.g., heme biosynthesis) are repressed during iron-depleted conditions by physical interaction of HapX with the CCAAT-binding core complex (CBC). Proteome analysis identified putative HapX targets. Mutual transcriptional control between *hapX* and *sreA* and synthetic lethality resulting from deletion of both regulatory genes indicate a tight interplay of these control systems. Expression of genes encoding CBC subunits was not influenced by iron availability, and their deletion was deleterious during iron-depleted and iron-replete conditions. Expression of *hapX* was repressed by iron and its deletion was deleterious during iron-depleted conditions only. These data indicate that the CBC has a general role and that HapX function is confined to iron-depleted conditions. Remarkably, CBC-mediated regulation has an inverse impact on the expression of the same gene set in *A. nidulans*, compared with *Saccharomyces cerevisae*.

The EMBO Journal (2007) **26,** 3157–3168. doi:10.1038/sj.emboj.7601752; Published online 14 June 2007
Subject Categories: chromatin & transcription; cellular metabolism

Keywords: CCAAT; Hap complex; iron; regulation; siderophore

*Corresponding authors. H Haas, Division of Molecular Biology, Biocenter, Innsbruck Medical University, Fritz-Pregl-Strasse 3, 6020 Innsbruck, Austria. Tel.: +43 512 9003 70205; Fax: +43 512 9003 73100; E-mail: hubertus.haas@i-med.ac.at
or AA Brakhage, Department of Molecular and Applied Microbiology, Leibniz Institute for Natural Product Research and Infection Biology (HKI), and Friedrich-Schiller-University Jena, Beutenbergstrasse 11a, 07745 Jena, Germany. Tel.: +49 3641 656601; Fax: +49 3641 656603; E-mail: axel.brakhage@hki-jena.de
[5]These authors contributed equally to this work

Received: 17 August 2006; accepted: 16 May 2007; published online: 14 June 2007

Introduction

The *cis*-acting sequence CCAAT is present in approximately 30% of eukaryotic promoters (Bucher, 1990). An evolutionarily conserved protein complex able to bind to this motif has been found in all eukaryotes analyzed so far, ranging from yeast to mammals. It has been designated Hap complex in *Saccharomyces cerevisiae* (Pinkham and Guarente, 1985; McNabb *et al*, 1995), *Kluyveromyces lactis* (Mulder *et al*, 1994), and *Arabidopsis thaliana* (Edwards *et al*, 1998), Php in *Schizosaccharomyces pombe* (McNabb *et al*, 1997), AnCF in *Aspergillus* species (reviewed in Brakhage *et al*, 1999), CBF in *Xenopus laevis* (Li *et al*, 1998), and NF-Y in mammals (Hooft van Huijsduijnen *et al*, 1990; Maity *et al*, 1990), respectively. The *S. cerevisiae* Hap complex was the first CCAAT-binding complex to be identified. It comprises four subunits, Hap2p, Hap3p, Hap4p and Hap5p. Hap2/3/5p form the core CCAAT-binding complex (here termed CBC), which is responsible for DNA binding, while Hap4p is involved in transcriptional activation (McNabb *et al*, 1995). Orthologs of Hap2/3/5p are present in all eukaryotes. Moreover, *S. cerevisiae* Hap2p, *A. nidulans* HapB and human NF-YA are functionally interchangeable (Becker *et al*, 1991; Tuncher *et al*, 2005), which demonstrates high evolutionary conservation of the CBC. However, with the exception of the yeast species *K. lactis* and *Hansenula polymorpha*, clear evidence for a Hap4p ortholog in other organisms is inconclusive (Bourgarel *et al*, 1999; Sybirna *et al*, 2005). In *S. cerevisiae*, the Hap4p/CBC complex acts as an activator of genes involved in oxidative phosphorylation in response to growth on non-fermentable carbon sources (Pinkham and Guarente, 1985). The *A. nidulans* CBC, consisting of the Hap2/3/5p orthologs HapB/C/E, modulates the expression of numerous genes, including the anabolic penicillin biosynthesis genes *acvA*, *ipnA* and *aatA* (Litzka *et al*, 1996; Then Bergh *et al*, 1996) and the catabolic acetamidase encoding *amdS* (Littlejohn and Hynes, 1992). In this respect it has also been shown that the activation of gene expression by pathway-specific regulators can depend on the presence of a functional CBC (Steidl *et al*, 1999). At the same time, evidence for CBC-mediated repression of gene expression was found in *A. nidulans* for homoaconitase-encoding *lysF* and in the auto-regulation of *hapB* expression (Steidl *et al*, 2001; Weidner *et al*, 2001). Recently, the CBC was also found to act as a repressor of mitochondrial electron transport components in *Candida albicans* (Johnson *et al*, 2005). However, a clear picture of the CBC regulon in fungi is missing so far.

A yeast-two-hybrid screen suggested physical interaction of *A. nidulans* HapB with a protein of a yet unknown function, termed HapX (Tanaka *et al*, 2002). HapX displays no similarity to *S. cerevisiae* Hap4p, apart from an N-terminal 17 amino-acid-motif, which has been shown to be essential for interaction of Hap4p with the *S. cerevisiae* CBC (McNabb and Pinto, 2005). Deletion of *hapX* in *A. nidulans* did not result in a slow-growth and weak-conidiation phenotype, as caused by a deletion of any of the three CBC subunit-encoding genes (Steidl *et al*, 1999). Furthermore, expression of *hapX* in *S. cerevisiae* did not complement the deletion of *Hap4*. Therefore, a function of HapX in CBC-mediated gene expression appeared unlikely at that time.

We resumed the functional analysis of *hapX*, as we found that its expression is repressed by iron via the GATA factor SreA. As a cofactor for numerous enzymes and in electron transport systems, iron is indispensable for all eukaryotes. However, an excess of iron is toxic, due to its capacity to catalyze the production of cell damaging reactive oxygen species (Halliwell and Gutteridge, 1984). Therefore, subtle control systems are required to maintain iron homeostasis. In *A. nidulans*, iron represses siderophore-mediated iron uptake, which is the major iron acquisition system and is essential for fungal virulence (Schrettl *et al*, 2004; Oide *et al*, 2006), and induces iron-dependent pathways (Haas *et al*, 1999; Oberegger *et al*, 2001, 2002b). The repression of the siderophore system under iron-replete (+Fe) conditions is mediated, at least in part, by SreA. Here, we demonstrate that HapX mediates repression of iron-dependent pathways under iron-depleted (−Fe) conditions via interaction with the CBC. HapX target genes were identified by a proteomic approach. The importance of a tight interplay between HapX and SreA is demonstrated by mutual transcriptional control between *hapX* and *sreA* and synthetic lethality resulting from deletion of both regulatory genes.

Results

Deletion of hapX or of genes encoding CBC subunits impedes growth during −Fe conditions

A differential mRNA display screen for SreA target genes (Oberegger *et al*, 2001) suggested that the steady-state level of *hapX* mRNA is repressed by iron in the wild type and partially derepressed in an *sreA* deletion (Δ) strain (data not shown). This expression pattern was confirmed using Northern analysis (Figure 1A). Notably, deletion of *sreA* results in about 30% derepression, which is typical for SreA target genes, for example, siderophore transporter-encoding *mirB* (Haas *et al*, 2003).

We compared the phenotypic consequences of *hapX* deletion during +Fe and −Fe conditions, because of the iron-dependent expression of *hapX*. Consistent with the previous analysis (Tanaka *et al*, 2002), during +Fe conditions, Δ*hapX* displayed no significant difference to a wild-type strain with respect to conidiation and growth rate on a solid medium (data not shown) and in a liquid medium (Table I). During −Fe conditions, however, the growth rate was significantly reduced in submerged cultures (Table I), and, on a solid medium, the mycelium was less dense and conidiation was severely impaired (data not shown). Ectopic integration of a functional *hapX* gene (strain $hapX^R$) cured these and all other defects of Δ*hapX* (Table I; Figure 2), which demonstrates that the Δ*hapX* phenotype is a direct result of the loss of HapX activity.

HapX was initially found to interact with the CBC subunit HapB. To ascertain a possible metabolic connection, we also compared the growth rates of strains lacking individual CBC subunits during +Fe and –Fe conditions. Deletion of *hapB*, *hapC* or *hapE* impairs growth during +Fe, as shown previously (Steidl *et al*, 1999), but in particular during −Fe conditions (Table I), which indicates a special function of the CBC during −Fe conditions consistent with a possible HapX/CBC interaction.

Deletion of hapX or of genes encoding CBC subunits causes accumulation of the iron-free heme precursor protoporphyrin IX (PpIX) during −Fe conditions

In contrast to the wild type, Δ*hapX,* Δ*hapB,* Δ*hapC* and Δ*hapE* mycelia displayed a red pigmentation concomitant with red auto-fluorescence during −Fe but not +Fe conditions (Figure 2A and B), which is typical for PpIX accumulation. Determination of the PpIX content revealed no significant difference between −Fe and +Fe conditions in the wild type (Figure 2C). In contrast, the PpIX content of Δ*hapX* increased slightly during +Fe conditions, and increased about 80-fold during −Fe conditions (Figure 2C and D). Moreover, the content of the PpIX precursors uroporphyrin, heptacarboxylporphyrin, hexacarboxylporphyrin, pentacarboxylporphyrin and coproporphyrin was significantly increased in Δ*hapX* during −Fe conditions (Figure 2D). Similarly, deletion of any of the CBC subunit-encoding genes caused a 20- to 50-fold increase in PpIX accumulation (Figure 2C).

Deletion of hapX or of genes encoding CBC subunits causes decreased extracellular and increased intracellular siderophore production

A. nidulans produces two major siderophores (Figure 1D), which are essential for growth (Eisendle *et al*, 2003); triacetylfusarinine C (TAFC) mobilizes extracellular iron and ferricrocin (FC) stores iron intracellularly (Eisendle *et al*, 2006). Because of the observed growth defect, we analyzed siderophore production in strains lacking HapX or CBC subunits (Figure 2E). During +Fe conditions, production of TAFC and FC was low and resembled the wild type in all strains (data not shown). During −Fe conditions, however, deletion of *hapX* or of any CBC subunit-encoding gene caused significantly decreased TAFC and increased FC production. Notably, the decrease in TAFC production was more pronounced in CBC subunit deletion mutants and FC accumulation was higher in a Δ*hapX* mutant.

Supplementation with iron-free TAFC to a final concentration of 20 μM only partially cured the growth defect of Δ*hapX* during −Fe conditions, whereas PpIX accumulation remained unaffected (data not shown). These data suggest that reduced TAFC production does not account for the full extent of growth reduction and PpIX accumulation resulting from *hapX* deletion.

HapX represses sreA expression without a general effect on the SreA regulon

To further investigate the altered siderophore production of Δ*hapX* and Δ*hapC* strains, we performed a Northern analysis of the known genes involved in siderophore metabolism

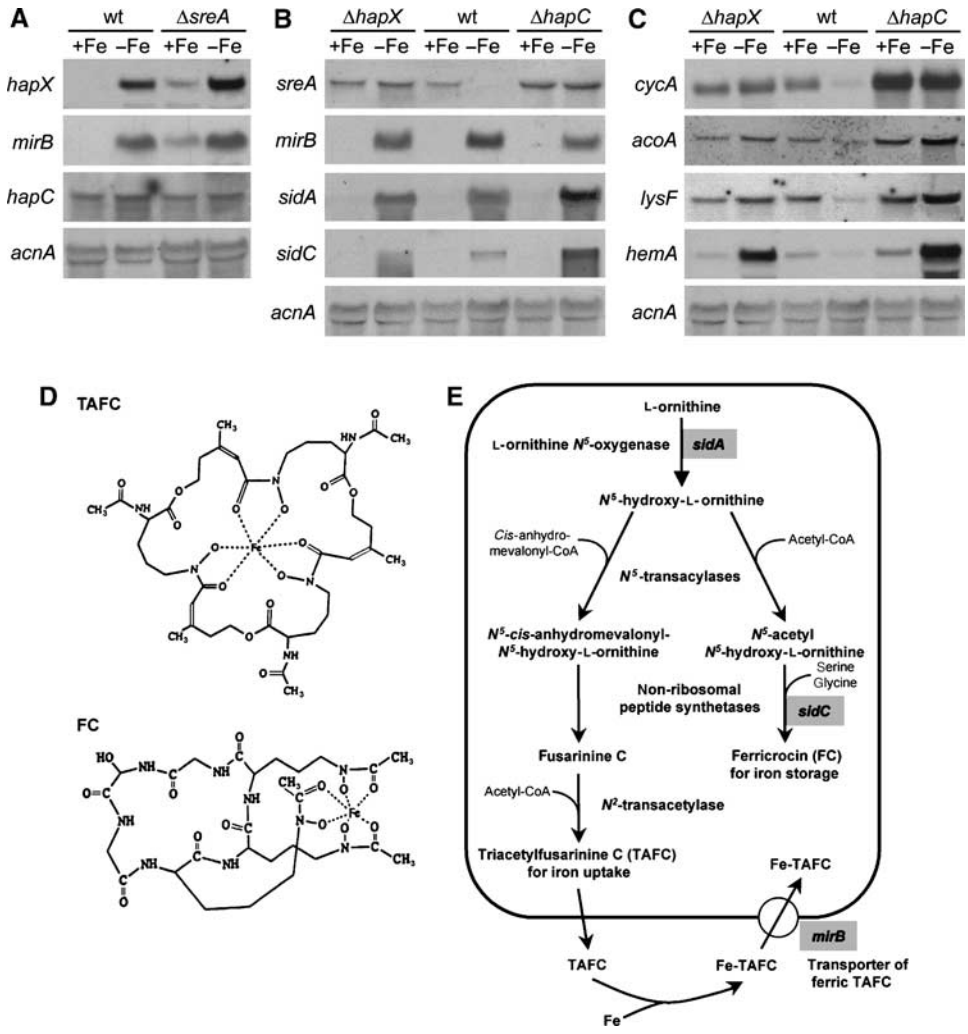

Figure 1 Iron-regulated gene expression in *A. nidulans* wild-type, Δ*sreA*, Δ*hapX* and Δ*hapC* strains. For Northern analysis, the total RNA was isolated from *A. nidulans* strains grown for 24 h under +Fe and −Fe conditions. As a control for loading and RNA quality, blots were hybridized with the γ-actin encoding *acnA* gene. (**A**) Expression of *hapX* but not *hapC* is partially controlled by SreA-mediated iron regulation. (**B**) Deletion of *hapX* or *hapC* causes derepression of *sreA*, during −Fe conditions but not the SreA regulon, during +Fe conditions. (**C**) Deletion of *hapX* or of *hapC* causes derepression of iron-dependent pathways during iron starvation. (**D**) *A. nidulans* siderophores. (**E**) *A. nidulans* siderophore metabolism. Known genes involved in siderophore biosynthesis and uptake are shaded in gray.

Table I Deletion of *hapX, hapB, hapC or hapE* causes a reduced growth rate during −Fe conditions

Strain	Growth condition		Ratio
	+Fe	−Fe	−Fe/+Fe
Wild type	100.0	66.9±8.4	0.67
Δ*hapX*	91.6±7.0	49.5±5.3	0.54
hapX^{R}	114.3±5.8	74.2±6.4	0.65
Δ*hapB*	46.3±5.9	23.7±3.1	0.51
Δ*hapC*	61.6±7.6	28.3±4.2	0.46
Δ*hapE*	54.6±6.3	25.5±2.7	0.47

Strains were grown for 24 h in –Fe and +Fe conditions. Dry weights were normalized to that of the wild type grown during iron-replete conditions, which was 0.58±0.04 g.

(Haas *et al*, 2003): *sreA* (repressor of siderophore metabolism), *mirB* (transporter for uptake of ferric TAFC), *sidA* (ornithine monooxygenase catalyzing the common step for biosynthesis of TAFC and FC) and *sidC* (non-ribosomal peptide synthetase required for FC synthesis) (Figure 1B). The proposed siderophore biosynthetic pathway is provided in Figure 1E.

As shown previously (Oberegger *et al*, 2002b), expression of *sreA* is repressed during −Fe conditions, whereas that of the SreA target genes *mirB*, *sidA*, and *sidC* is repressed during +Fe conditions. Deletion of *hapX* or of *hapC* caused derepression of *sreA* during −Fe conditions (Figure 1B). In turn, as SreA represses siderophore biosynthesis and uptake, it was conceivable that SreA-regulated genes were repressed during −Fe conditions in these strains. However, regulation of *mirB* and *sidA* was unaffected in both Δ*hapX* and Δ*hapC* and, therefore, does not explain the reduced TAFC production. These data suggest that SreA-mediated repression requires either post-translational activation, and/or other additional factors. In contrast, the transcript levels of *sidC* were elevated in Δ*hapX* and Δ*hapC* during −Fe conditions, which agrees with the increased FC accumulation. Notably, *sidC* transcripts are approximately 15 kb in length and are therefore preferentially subject to physical degradation during RNA preparation. The upregulation of *sidC* expression in Δ*hapX* was also confirmed by dot blot analysis (data not shown).

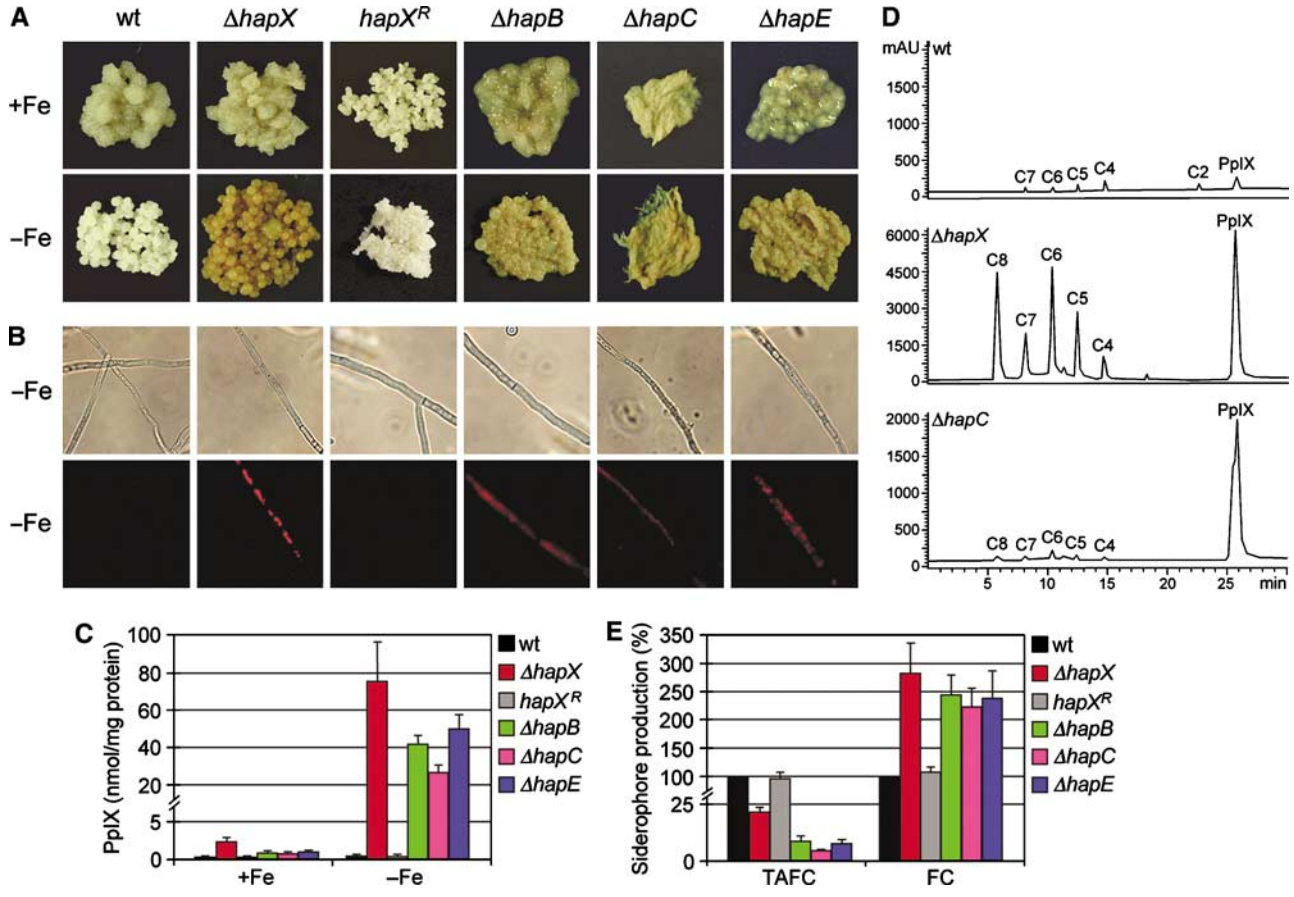

Figure 2 Deletion of hapX or genes encoding CBC subunits leads to cellular accumulation of PpIX, decreased TAFC synthesis and increased FC production, during −Fe conditions. (**A**) Mycelia of *A. nidulans* strains after growth for 24 h during + Fe and –Fe conditions. (**B**) Characteristic red auto-fluorescence caused by PpIX accumulation during −Fe conditions. During + Fe conditions, no auto-fluorescence was detectable in any strain (data not shown). (**C**) Quantification of PpIX accumulation. (**D**) Representative chromatograms of porphyrin analysis of wild-type, Δ*hapX* and Δ*hapC* strains after growth under −Fe conditions. C8, C7, C6, C5, C4 and C2 denote uroporphyrin, heptacarboxylporphyrin, hexacarboxylporphyrin, pentacarboxylporphyrin, coproporphyrin and protoporphyrin, respectively. (**E**) Quantification of siderophore production during −Fe conditions normalized to that of the wild type. The data represent the mean ± s.d. of three simultaneously harvested flasks.

HapX and the CBC are required to repress iron-dependent pathways during –Fe conditions

sreA belongs to a class of genes, which are downregulated during iron starvation. Most members of this class encode proteins requiring iron-containing cofactors, such as *cycA*, which encodes the heme-protein cytochrome *c*, as well as *acoA* and *lysF*, which encode the iron–sulfur cluster proteins aconitase and homoaconitase, respectively (Oberegger *et al*, 2002a). Another example is *hemA*, which codes for 5-aminolevulinate synthase (Bradshaw *et al*, 1993). HemA does not require iron by itself, but catalyzes the first committed step in heme biosynthesis. Deletion of *hapX* or of CBC subunit-encoding genes resulted in derepressed expression of all four genes during –Fe conditions (Figure 1C). In agreement with PpIX accumulation (Figure 2C), *hemA* expression was not only derepressed, but highly upregulated in both Δ*hapX* and Δ*hapC* (Figure 1C). A hypothetical explanation for the latter would be the lack of feedback inhibition of *hemA* expression by heme. Remarkably, *hapC* deletion resulted not only in derepression of iron-dependent pathways during −Fe conditions, but additionally in their upregulation during + Fe growth, in particular that of *cycA* (Figure 1C).

Notably, neither *sreA* (Figure 1A) nor *hapX* deletion affected the *hapC* transcript levels, and *hapC* deletion did not affect *hapX* expression (data not shown).

The *A. nidulans* wild-type BPU used is auxotrophic for uracil (*pyrG89*) and pyridoxamine (*pyroA4*). With respect to siderophore production and PpIX accumulation, BPU did not show any difference to *A. nidulans* strain TRAN, which is prototrophic for uracil and pyridoxamine, demonstrating that these auxotrophies do not influence iron metabolism (data not shown). Consistently, regulation of siderophore biosynthesis and iron-dependent pathways in BPU was as previously shown in TRAN (Oberegger *et al*, 2002a, b).

Interaction of HapX with DNA-bound CBC is abolished by iron

To investigate putative HapX/CBC interaction *in vivo*, we applied bimolecular fluorescence complementation (BiFC) assays, previously shown to be valuable to define *in vivo* protein interaction (Hink *et al*, 2002; Hu and Kerppola, 2003; Hoff and Kück, 2005). BiFC was detected between enhanced-yellow-fluorescent-protein (eYFP) split fragments fused to HapX and HapB in strain *yXB*, under −Fe (Figure 3B) but not + Fe conditions (Figure 3A). BiFC could not be detected between HapX and HapB in the Δ*hapC* strain *yXB*Δ*C* (Figure 3C), but was reconstituted by complementation with the *hapC* gene in strain *yXBC*^{c} (Figure 3D). Northern analysis confirmed constitutive expression of the two eYFP split fragment-encoding genes in the used strains

(Supplementary Figure 1). These data indicate that the entire CBC is required for *in vivo* interaction with HapX.

HapE contains two evolutionary conserved regions (Figure 4A). Domain B is conserved among all HapE orthologs and is essential for the assembly of the CBC, as shown for *S. cerevisiae* Hap5p (McNabb *et al*, 1997). In contrast, domain A is only conserved among fungal HapE orthologs and has been shown to be required for the recruitment of Hap4p in *S. cerevisiae*. Recently, Tanoue *et al* (2006) reported that only the B-domain is required for CBC-mediated transcriptional activation in *A. nidulans*. Here, we found that deletion of the non-conserved N-terminal region and the A-domain phenocopies *hapX* deletion, that is, wild type-like growth during +Fe conditions, but decreased growth rate, reduced TAFC production, and increased accumulation of FC and PpIX during −Fe conditions (Figure 4B). In contrast, truncation of the non-conserved C-terminal domain of HapE had no effect (Figure 4B). These data suggest that the region encompassing the N-terminus and the A-domain of HapE is involved in interaction with HapX *in vivo*.

The 5′-upstream regions of the putative HapX/CBC target genes *cycA*, *acoA*, *lysF*, *hemA* and *sreA* all contain CCAAT boxes (Supplementary Figure 2). To study interaction of the CBC with the CCAAT sequences from promoter regions of iron-induced genes, we overproduced recombinant HapB, HapC, HapE, HapE-ΔNΔA and HapX in *Escherichia coli* and purified the proteins to homogeneity (Figure 5A). The CBC was reconstituted by mixing equimolar amounts of the CBC subunits. Real-time protein–DNA interaction analysis was performed with two 50-bp DNA duplexes immobilized on flow cells of a surface plasmon resonance (SPR) biosensor. The two sequences used covered the CCAAT box at position −1235 of the *sreA* promoter, which perfectly matches the consensus CBC-binding sequence (Mantovani, 1998), and the CCAAT box at position −181 of the *lysF* promoter, respectively. The apparent dissociation constants of the CBC were 1.8 and 4.6 nM for the CCAAT boxes from *sreA* and *lysF*, respectively, indicating specific and high-affinity binding.

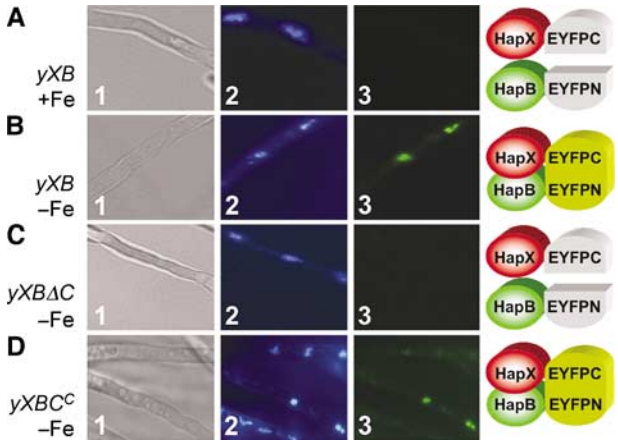

Figure 3 HapX and HapB interact *in vivo*. The interaction was observed after 24 h of growth, using BiFC in *A. nidulans* strains producing HapX and HapB fused with the C-terminal and N-terminal split fragments of eYFP, respectively. Panels 1, light microscopy; panels 2 and 3, fluorescence microscopy of DAPI-stained nuclei and BiFC, respectively. HapX and HapB interact during −Fe (**B**) but not +Fe (**A**) conditions in strain *yXB*. (**C**) HapX/HapB interaction is abolished by deletion of *hapC* in strain *yXBΔC* and is (**D**) reconstituted after complementation of *yXBΔC* with *hapC* in *yXBC^c*.

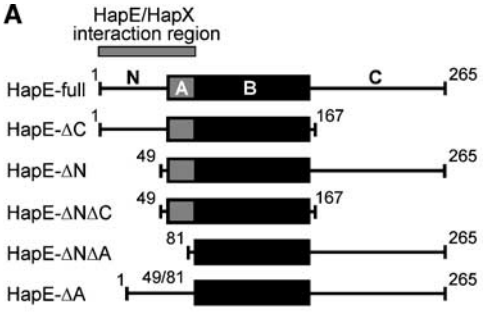

B

Strain	Dry weight (%)		Ratio	−Fe		
	+Fe	−Fe	−Fe/+Fe	TAFC (%)	FC (%)	PpIX[2]
Wild type	100.0[1]	62.4 ± 7.9	0.62	100.0	100.0	0.3 ± 0.1
Δ*hapX*	103.7 ± 4.7	35.4 ± 1.2	0.34	25.7 ± 3.6	278.8 ± 59.0	63.6 ± 12.3
hapE-full	104.9 ± 13.1	69.2 ± 9.1	0.66	99.8 ± 9.3	112.3 ± 6.8	0.2 ± 0.1
hapE-ΔC	106.8 ± 5.5	71.6 ± 3.9	0.67	92.0 ± 5.2	118.5 ± 13.3	0.1 ± 0.1
hapE-ΔN	113.3 ± 11.6	38.8 ± 4.2	0.34	55.6 ± 6.1	175.7 ± 8.7	54.1 ± 8.5
hapE-ΔNΔC	105.4 ± 11.9	38.1 ± 2.9	0.36	66.4 ± 7.9	246.4 ± 45.8	46.3 ± 5.1
hapE-ΔNΔA	108.4 ± 8.3	29.7 ± 2.5	0.27	25.8 ± 4.7	263.7 ± 37.9	59.9 ± 14.2
hapE-ΔA	112.7 ± 7.1	35.3 ± 3.2	0.31	23.7 ± 1.6	267.9 ± 43.2	61.3 ± 13.5

[1] Dry weights were normalized to that of the wild type grown during +Fe conditions (1.02±0.11 g).
[2] PpIX is given in nmol/mg protein.

Figure 4 Deletion of the non-conserved N-terminal region or the conserved A-domain of HapE phenocopies *hapX* deletion. (**A**) Schematic representation of the HapE versions investigated. (**B**) Growth rates and production of TAFC, FC and PpIX after growth for 48 h during + Fe and −Fe conditions. For induction of amylase promoter-driven genes (Tanoue *et al*, 2006), strains were grown in medium containing starch as the sole carbon source. During +Fe conditions, production of TAFC, FC and PpIX was wild type-like in all strains (data not shown).

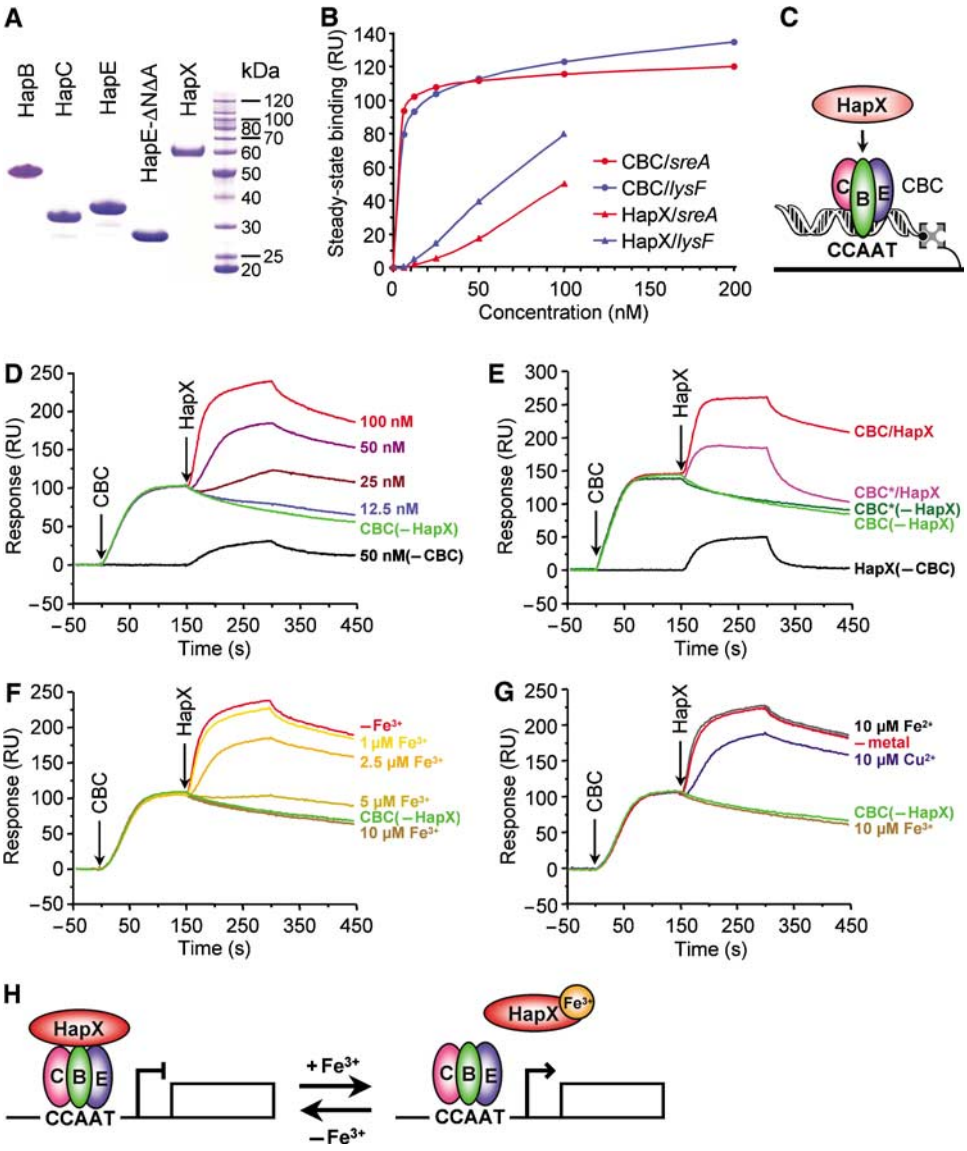

Figure 5 SPR analysis of iron-regulated HapX binding to DNA-bound CBC. (**A**) SDS–PAGE analysis of 1.5 μg of purified HapB, HapC, HapE, HapE-ΔNΔA and HapX proteins. (**B**) Concentration-dependent, steady-state binding of the CBC to biosensor-bound CCAAT boxes derived from the 5′-upstream regions of *sreA* and *lysF*, respectively. (**C**) Schematic representation of the SPR analysis of HapX/CBC interaction. HapX was injected onto preformed CBC/DNA complexes after reaching the steady-state level (**D**) Concentration-dependent association of HapX (12.5, 25, 50 and 100 nM, respectively) to the CBC (6.25 nM) bound to the biosensor-linked *sreA* CCAAT box. 'CBC(−HapX)' shows the steady-state association of the CBC to the CCAAT box without application of HapX. '(−CBC)' shows the unspecific interaction of HapX (50 nM) with sensor-bound DNA. (**E**) Comparison of the interaction of HapX (100 nM) with the CBC and with the CBC containing HapE-ΔNΔA (CBC*). Note that 12.5 nM CBC* was necessary to reach an equilibrium response equivalent to 6.25 nM CBC. (**F**) Interaction of HapX (100 nM) after preincubation with iron (1, 2.5, 5 and 10 μM $FeCl_3$, respectively) or without iron (−Fe), with the DNA-bound CBC (6.25 nM). (**G**) Interaction of HapX (100 nM) after preincubation with 10 μM $FeCl_3$, 10 μM $(NH_4)_2Fe(SO_4)_2$, 10 μM $CuCl_2$, or without any metal (−metal), with DNA-bound CBC (6.25 nM). (**H**) Proposed model for HapX/CBC-mediated regulation of iron-dependent pathways and *sreA*.

In contrast, HapX alone bound non-specifically, and with low affinity to sensor-bound DNA. (Figure 5B).

To investigate HapX/CBC interaction *in vitro*, HapX was injected onto the preformed CBC/DNA complex after reaching the steady-state level, as represented schematically in Figure 5C. Apart from its unspecific DNA binding, HapX bound with a remarkably high affinity to the CBC bound to the CCAAT box from the *sreA* promoter (Figure 5D). However, HapX did not bind to a CBC containing a HapE version that lacks the N-terminal region and the A-domain (HapE-ΔNΔA), that is, the measured response did not exceed the unspecific interaction of HapX with CBC-free DNA (Figure 5E). The latter agrees with the *in vivo* requirement for the N- and A-domains of HapE for repression of iron-dependent pathways during −Fe conditions (Figure 4B). Consistent with the observed lack of interaction between HapX and the CBC during +Fe conditions *in vivo*, the *in vitro* interaction was abolished upon preincubation of HapX with Fe^{3+} (Figure 5F). Notably, the interaction of HapX with the CBC was not abolished by preincubation with the same concentration of Fe^{2+} or Cu^{2+}, indicating that the Fe^{3+} effect is specific (Figure 5G).

Identification of putative HapX targets

To identify other possible targets for HapX-dependent regulation, we examined the global effect of *hapX* deletion at

the proteomic level. For this purpose, protein extracts of wild-type and Δ*hapX* strains grown for 19 h during −Fe conditions were compared by 2D-PAGE (Supplementary Figure 3). Reproducibly, 19 proteins displayed an increase and 23 proteins a decrease in their levels of more than 1.8-fold in the Δ*hapX* mutant. Some proteins appeared in gels as more than one spot with the same apparent molecular mass, but with different pI values and abundance, presumably due to post-translational modifications or isoenzyme variation, for example, 3-isopropylmalate dehydratase. Therefore, the 42 spots identified represented only 30 different proteins (Table II). Increased levels of 5-aminolevulinic acid synthase (HemA) and aconitase (AcoA) in Δ*hapX* agreed with the transcriptional upregulation of the encoding genes (Figure 1C). Further iron-related proteins with increased levels in Δ*hapX* during −Fe conditions were iron–sulfur cluster containing 3-isopropylmalate dehydratase, iron-containing 3-deoxy-D-arabino-heptulosonate-7-phosphate synthase, the mitochondrial processing peptidase, the respiratory protein ATP synthase subunit D, and the respiratory heme-proteins cytochrome *c* peroxidase, and ubiquinol–cytochrome *c* reductase complex core protein 2. This finding suggests that the encoding genes are further targets for HapX-mediated repression. Moreover, deletion of *hapX* also resulted in decreased levels of some proteins, for example, several dehydrogenases, oxidoreductases and proteins involved in amino-acid metabolism.

Deletion of sreA in combination with deletion of hapX or of hapB is lethal

To address the role of HapX in iron metabolism, we attempted to generate a mutant lacking both *hapX* and *sreA*, via a meiotic cross of strains Δ*hapX* and Δ*sreA*. With arginine supplementation, 26% of the progeny were hapX$^+$/sreA$^+$ recombinants, 40% *hapX*$^+$/Δ*sreA* and 34% Δ*hapX/sreA*$^+$; however, Δ*hapX*/Δ*sreA* recombinants were not recovered (Supplementary Table 1). Without arginine supplementation, hapX$^+$/sreA$^+$ recombinants cannot grow, due to the *argB2* mutation of both parental strains. Because *hapX* and *sreA* are located on different chromosomes (II and VIII, respectively), 33% of the progeny was expected to be Δ*hapX*/Δ*sreA* double mutants. Among the 50 randomly chosen progeny screened by PCR (Supplementary Table 2), 27 had a Δ*hapX/sreA*$^+$ genotype and 23 had a *hapX*$^+$/Δ*sreA* genotype, but again Δ*hapX*/Δ*sreA* double mutants could not be recovered. The probability of not recovering the Δ*hapX*/Δ*sreA* double mutant without arginine supplementation is $(1–0.33)^{50}$, or 2.0×10^{-9}. In both cases, the three additional genetic markers (*pyroA4, pyrG89* and *wA3)* segregated according to the Mendelian rules (Supplementary Table 1). These results strongly suggest that the deletion of both *hapX* and *sreA* is lethal.

To test the genetic interaction between SreA and the CBC, we generated a strain, designated Δ*sreA*/Δ*hapB/hapB*^{c}, that contained deletions of the *sreA* and *hapB* loci along with an ectopic copy of the *hapB* gene controlled by the *alcA* promoter, by meiotically crossing strains Δ*sreA* and Δ*hapB/hapB*^{c} (Steidl *et al*, 2004). Under inducing conditions, Δ*sreA*/Δ*hapB/hapB*^{c} showed growth comparable to Δ*sreA*. In contrast, no growth was observed under conditions that cause repression of the *alcA* promoter, supporting the synthetic lethal interaction also between SreA and the CBC (data not shown).

Discussion

All organisms face constantly changing availability of the essential metal, iron. To avoid deleterious consequences caused by iron overload, as well as iron deficiency, organisms have evolved mechanisms that maintain iron homeostasis. During iron deprivation, *A. nidulans* cells undergo a transcriptional remodeling, leading to the inverse regulation of two major sets of genes. On one hand, iron acquisition, for example, siderophore-mediated iron uptake, is upregulated (Haas, 2003). On the other hand, many iron-dependent pathways, including proteins involved in the tricarboxylic acid cycle, respiration and heme biosynthesis, are downregulated (Oberegger *et al*, 2002a). The latter pathways represent oxidative metabolism, which largely depends on iron.

We show that various iron-dependent pathways are repressed during −Fe conditions, by the interaction of HapX with the CBC. The lines of evidence are: (i) *hapX* and CBC subunit-encoding genes are required for repression of genes involved in oxidative metabolism during −Fe conditions and their deletion causes PpIX accumulation; (ii) HapX physically interacts with the CBC *in vitro* and *in vivo* only under –Fe conditions; (iii) HapX/CBC binds to the CCAAT boxes of at least two HapX/CBC target genes, *sreA* and *lysF*; (iv) the non-conserved N-terminal region and the A-domain of HapE are required for *in vitro* interaction of the CBC with HapX. In agreement, strains carrying HapE versions with N-terminal deletions phenocopy *hapX* deletion *in vivo*.

Proteome analysis confirmed some of the HapX/CBC targets detected by transcriptional analysis, identified some more obviously iron-related targets, and revealed putative HapX targets not previously shown to be affected by iron metabolism. Moreover, we found that HapX/CBC formally acts as a repressor of TAFC production, but not via transcriptional control of known siderophore biosynthesis genes, and as a repressor of FC production, which agrees with increased transcript levels of FC-biosynthetic *sidC* in Δ*hapX* and Δ*hapC* mutants.

Deletion of *hapX* is deleterious only during −Fe conditions. In contrast, deletion of genes encoding CBC subunits has deleterious consequences during both +Fe and −Fe conditions. Consistently, expression of *hapX* is confined to −Fe conditions, but that of the CBC subunit-encoding genes is constitutive, which is achieved by negative auto-regulation of the *hapB* gene (Steidl *et al*, 2001). Furthermore, *hapB* deletion is epistatic to *hapX* deletion, that is, a Δ*hapX*/Δ*hapB* double mutant displayed a phenotype identical to Δ*hapB* (data not shown). HapX-independent functioning of the CBC is also indicated by the CBC-independent nuclear localization of HapX (Goda *et al*, 2005), that is, HapC and HapE, but not HapX, depend on a HapB-mediated 'piggy-back' nuclear transport (Steidl *et al*, 2004). Moreover, deletion of *hapC*, but not of *hapX*, caused upregulation of iron-dependent pathways during +Fe conditions. Together, these data show that the CBC has a role independent of the iron status, whereas HapX/CBC function appears to be confined to −Fe conditions. The more general effect of the CBC on gene regulation, compared to HapX/CBC, is probably also the explanation for the different extent of deregulation of TAFC, FC and PpIX production in *hapX* and CBC subunit-encoding gene deletion strains.

In *C. albicans,* CBC-mediated repression of respiration was reported (Johnson *et al*, 2005), and a putative ortholog of

Table II Comparison of the proteome of the wild type and Δ*hapX* during −Fe conditions

Putative function	Locus	pI/MW	Spot	Fold changes	Sequence coverage (%)	Identified peptides	Mascot score
(A) Proteins with higher levels in ΔhapX versus wild type							
3-Isopropylmalate dehydratase	AN5886.2	5.5/84	1	+2.9	20	8	109
			2	+2.6	14	6	89.5
			3	+1.7	35	12	166
			4	+3.5	44	14	211
			5	+3.4	35	12	171
			6	+2.3	37	12	124
Aconitate hydratase, mitochondrial	AN5525.2	5.9/83	7	+2.1	17	8	95
			8	+2.0	39	17	177
			9	+1.7	26	12	95.7
Cytochrome *c* peroxidase, mitochondrial precursor	AN1630	9.4/40	12	+1.9	34	8	80.7
Ubiquinol–cytochrome *c* reductase complex core protein 2	AN8273.2	9.4/48	13	+1.8	16	5	58.3
5-Aminolevulinic acid synthase	AN2284.2	9.5/69	14	+19.2	21	8	118
		9.5/69	15	+2.1	30	10	160
		9.5/69	16	+2.5	34	8	188
Phe-inhibited 3-deoxy-D-arabino-heptulosonate-7-phosphate synthase (DAHP)	AAG36950	6.6/40	18	+1.7	28	6	88.6
ATP synthase D chain, mitochondrial	AN6631.2	7.2/20	22	+3.1	49	4	98.3
Cobalamin-independent methionine synthase	AAF82115	6.4/87	27	+13.7	31	15	194
Phosphoribosylaminoimidazolecarboxamide for myltransferase/IMP cyclohydrolase	AN4464.2	6.2/66	29	+5.1	31	9	185
Predicted RNA-binding protein	AN1044.2	4.3/66	30	+3.1	21	4	82
Mitochondrial processing peptidase β subunit	AN0747.2	5.5/53	31	+2.3	33	8	105
RNA recognition motif	AN6004.2	5.6/29	32	+6.3	40	6	136
(B) Proteins with lower levels in ΔhapX versus wild type							
NADH-ubiquinone oxidoreductase 75 kDa subunit	AN9411.2	6.0/81	10	−2.1	31	9	181
Fe-containing alcohol dehydrogenase	AN1868.2	6.9/53	11	−2.6	19	6	63.6
3-Hydroxy-3-methylglutaryl CoA synthase	AN4923.2	5.8/51	17	−2.0	32	7	101
Aspartic protease	AN2903.2	4.7/43	19	−3.0	26	5	76.4
Aminotransferase, classes I and II	AN5591.2	5.7/54	20	−2.1	18	6	89.6
Woronin body major protein	AN4695.2	6.8/25	21	−3.2	51	3	101
Hydantoinase/oxoprolinase	AN5652.2	5.2/141	23	−3.5	29	17	260
			24	−2.2		—	—
			25	−3.3	34	17	329
			26	−2.7	40	20	351
Proteasome alpha subunit	AN4869.2	6.7/28	28	−2.0	52	8	150
GMC oxidoreductase	AN3206.2	5.4/63	33	−2.7	16	6	91.3
UDP-glucose pyrophosphorylase	AAW49005	7.9/58	34	−2.3	39	12	157
Alcohol dehydrogenase, zinc containing	AN8406.2	6.0/38	35	−2.2	53	7	169
Alcohol dehydrogenase, zinc containing	AN0443.2	6.2/40	36	−2.0	56	10	189
Haloacid dehalogenase-like hydrolase	AN4572.2	5.7/36	37	−3.9	30	5	81
Carboxyphosphonoenolpyruvate phosphonomutase	AN3805.2	5.6/32	38	−6.5	49	8	133
L-Xylulose reductase	AN7590.2	6.4/28	39	−3.4	56	8	120
Oxidoreductase, short-chain dehydrogenase/reductase family	AN3161.2	9.6/37	40	−4.1	29	7	91.4
Transcription initiation factor subunit TAF30	AN0083.2	8.7/35	41	−2.6	25	5	82.6
Hypothetical protein	AN1152.2	5.4/19	42	−2.8	50	3	72.8

HapX was found to be subject to iron regulation mediated by Sfu1, the ortholog of *A. nidulans* SreA (Lan *et al*, 2004). Recently, mutual transcriptional control of the SreA ortholog Fep1 and Php4, which displays similarity to the *S. cerevisiae* Hap4p in the N-terminus, was found in *S. pombe* (Mercier *et al*, 2006). Moreover, Php4 and the CBC were shown to be required for repression of some iron-dependent pathways during −Fe conditions, but, in contrast to *A. nidulans*, the CBC is also required for transcriptional upregulation of the respective genes during +Fe conditions in this yeast. Nevertheless, these data indicate evolutionary conservation of HapX/CBC-mediated repression of oxidative metabolism in other fungal species. In striking contrast, in *S. cerevisiae*, the Hap4p/CBC complex acts as an inducer of oxidative metabolism (Pinkham and Guarente, 1985). In particular, the genes encoding cytochrome *c,* aconitase and 5-aminolevulinate synthase, which are repressed by the CBC in *A. nidulans*, are positively influenced in *S. cerevisiae* (Keng and Guarente, 1987; Pinkham *et al*, 1987; Liu and Butow, 1999). The downregulation of iron-dependent pathways in *S. cerevisiae* occurs by acceleration of the rate of mRNA decay, which is mediated by the RNA-binding protein Cth2p/Tis11p (Puig *et al*, 2005). Orthologs of Cth2p/Tis11p appear to be missing in the genomes of *A. nidulans* and all other filamentous fungal species. Taken together, these results suggest fundamental differences in the regulation of oxidative metabolism between *S. cerevisiae* and other fungi.

Intimate coupling of the regulatory mechanisms mediating the inverse regulation of iron-dependent pathways and iron acquisition systems is suggested by the synthetic lethality of double deletion of *sreA* and *hapX*, as well as of *sreA* and *hapB*. The requirement of at least one of these regulatory circuits suggests mutual compensation of essential functions. A tight interplay is further indicated by mutual transcriptional control between SreA and HapX. Here, we have shown that *in vitro* HapX/CBC binds to the *sreA* promoter, and SreA is able to bind to GATA sites of the *hapX* promoter (data not shown). However, the deregulation of *hapX*, as well as of *sreA*, had no impact on the regulation of the respective target genes. In agreement with these results, we have previously shown that constitutive expression of *sreA* does not repress siderophore biosynthesis (Haas *et al*, 1999), and the same is true for HapX targets in a strain constitutively expressing *hapX* (data not shown). These data suggest that the repressor function of both SreA and HapX/CBC requires additional factors and/or post-transcriptional modification. SreA might sense the iron status by an evolutionarily conserved cysteine-rich region, as suggested for other fungal SreA orthologs (Harrison and Marzluf, 2002; Pelletier *et al*, 2005). Remarkably, the putative HapX orthologs of *Neurospora crassa*, *C. albicans* and *Cryptococcus neoformans* also contain evolutionarily conserved cysteine-rich regions (although of different architecture as in SreA), which might be involved in sensing of iron (Supplementary Figure 4). Consistently, we found that *in vitro* and *in vivo* interaction of HapX with the CBC is abolished by iron. Taken together, these data suggest the following model (Figure 5H), in which HapX/CBC interaction is regulated at both transcriptional and post-translational levels. Iron starvation causes expression of *hapX*. Subsequent binding of HapX to the CBC results in transcriptional repression of iron-dependent pathways. During +Fe conditions, *hapX* is repressed and, therefore, iron-dependent pathways are derepressed. Moreover, HapX/CBC interaction is inhibited by increased iron concentrations. This post-translational mechanism allows rapid adjustment to iron availability by disruption of the HapX/CBC complex. In this respect it is interesting to note that the iron content of *A. nidulans* increases about 86-fold to approximately $20\,\mu mol\,g^{-1}$ fungal dry weight during a shift from −Fe to +Fe conditions (Eisendle *et al*, 2006). Mutual transcriptional control of *hapX* and *sreA* coordinates iron acquisition and iron-dependent pathways, thereby serving for both iron supply and prevention of iron toxicity.

It will be interesting to analyze how iron directly influences the binding affinity of HapX to the CBC. As mentioned above, HapX contains three cysteine-rich domains, which are potential ligands for this metal. In comparison, *S. cerevisiae* Hap4p displays similarity to HapX in the N-terminal region, which interacts with the CBC, but lacks the bZip domain and cysteine-rich motifs (Tanaka *et al*, 2002).

In contrast to oxidative metabolism, utilization of secondary carbon and nitrogen sources (e.g., acetamide, formamide, γ-aminobutyrate and starch), as well as the production of the secondary metabolite penicillin are positively regulated by the CBC in *Aspergillus* (Brakhage *et al*, 1999; Kato, 2005). This might indicate that CBC-mediated regulation coordinates oxidative metabolism, utilization of secondary carbon and nitrogen sources, as well as secondary metabolism.

Materials and methods

Strains, oligonucleotides, media and growth conditions

The *A. nidulans* strains and oligonucleotides used in this study are listed in Table III and Supplementary Table 2, respectively. Generally, fungal strains were grown at 37°C in *Aspergillus* minimal medium (AMM), according to Pontecorvo *et al* (1953), containing 1% (w/v) glucose as the carbon source, 20 mM glutamine as the nitrogen source, 10 μM $FeSO_4$ as the iron source and the respective supplements (+Fe conditions). Addition of iron was omitted for creating −Fe conditions. BiFC analyses were performed after growth of fungi on coverslips submerged in liquid medium. Under these conditions, biomass production is low and therefore additional treatment with 1 mM deferoxamine mesylate salt for 1 h was essential to cause iron starvation. The amylase promoter of *hapE* versions and the *alcA* promoter were induced using AMM with 1% (w/v) starch and with 3% (w/v) lactose plus 10 mM threonine as the carbon source, respectively. For repression of the *alcA* promoter, 1% (w/v) glucose was used. Shake flask culture (180 r.p.m.) included inoculation of 10^8 conidia in 200 ml of medium, in 1.0 l Erlenmeyer flasks.

Complementation of ΔhapX

A. nidulans $hapX^R$ was generated by ectopic integration of a single copy of the *hapX*-containing plasmid pCAME703-AoHapX-full (Goda *et al*, 2005), via co-transformation with plasmid pSK275, which carries the pyrithiamine resistance gene *ptrA*. The screening was performed by selection for pyrithiamine resistance and *hapX* integration by PCR (primer: o1_ hapX/o3_ hapX and o3_ hapX/o2_ argB) as well as Southern analysis.

Northern analysis, siderophores analysis and sexual crosses

Northern analysis as well as purification and analysis of TAFC and FC were carried out as previously described (Oberegger *et al*, 2001). Sexual crosses were performed according to Pontecorvo *et al* (1953).

Fluorescence analysis, PpIX analysis

Red auto-fluorescence was visualized with a Zeiss Axioplan fluorescence microscope with appropriate filters (excitation/emission at 546/590 nm). A digital Zeiss Axiocam MRc camera (Carl Zeiss AG) was used for documentation. Porphyrins were quantified by HPLC with UV and fluorescence detection, according to Bonkovsky *et al* (1986), and normalized to the sample protein content.

For all other fluorescence microscopic studies, a Leica DM4500 B digital fluorescence microscope (Leica Microsystems) was employed, using filtercubes A, GFP and YFP for nuclear staining, GFP localization studies and BiFC analysis, respectively. Nuclei were stained with 4′,6-diamidino-2-phenylindol (DAPI) for 1 min. For documentation, a Leica DFC480 digital camera (Leica Microsystems) was used. Photographs were processed with Photoshop 5.5 (Adobe Systems).

Proteome analysis

Proteome analysis of *A. nidulans*, including sample preparation, 2D-chromatography, protein visualization, quantification and MS identification of proteins, was essentially carried out as previously described for *A. fumigatus* (Kniemeyer *et al*, 2006). Gel images ($n=12$) were analyzed using the software Delta 2D 3.3 (Decodon). Afterwards, background subtraction spot volumes were normalized against total spot volume and total spot area. Spot values were logarithmically transformed and regarded as differentially regulated with a *t*-test value $P<0.05$. The MALDI-TOF data were used to search the NCBI database, using the Mascot algorithm (Matrix Science), with the following parameters: Cys as *S*-carbamidomethyl derivative and Met in oxidized form (variable), one missed cleavage site, peptide mass tolerance of 200 ppm.

Purification of HapB, HapC, HapE, HapE-ΔNΔA and HapX

Genes encoding N-terminally $(His)_6$-tagged versions of full-length HapX, HapB, HapE and a HapE version with a deletion of the first 80 amino acids (HapE-ΔNΔA) were expressed using vector pET-43.1a (Novagen). A gene encoding full-length HapC with an extended N-terminus including maltose-binding protein (MBP), a $(His)_6$ tag and a cleavage site for tobacco etch virus (TEV) protease was expressed using vector pMAL-c2X (New England Biolabs). All recombinant

Table III Fungal strains used in this study

Strain designation in text	Strain	Genotype	Reference
Gene regulation, synthetic lethality, epistasis			
Wild type	BPU1	*pyrG89*; *biA*; *wA3*; *argB2*; *pyroA4*; pAR5 (*argB*); ArgB$^+$	Tanaka *et al* (2002)
Wild type	TRAN	*argB2*; *bgA0*; *biA1*; *argB2*::pTRAN; ArgB$^+$	Haas *et al* (2003)
Δ*sreA*	SRKO1	*argB2*; *bgA0*; *biA*; *sreA*Δ::*argB*; ArgB$^+$	Haas *et al* (1999)
Δ*hapB*	ΔB-HapEegfp	*pyrG89*; *pabaA1*; *fwA1*; *hapB*Δ::*argB*; pHapE-GFP; PyrG$^+$	Steidl *et al* (2004)
Δ*hapC*	Nat24	*pyrG89*; *pabaA1*; *riboB*; *hapC*Δ::*riboB;* RiboB$^+$	Steidl *et al* (2004)
Δ*hapE*		*pyrG89*; *biA*; *wA3*; *argB2*; *pyroA4*; *pabaA1*; *hapE*Δ::*argB*; pTG-Taa; PyrG$^+$; ArgB$^+$	Tanoue *et al* (2006)
Δ*hapX*	BPUΔX1	*pyrG89*; *biA*; *wA3*; *argB2*; *pyroA4*; *hapX*Δ::*argB;* ArgB$^+$	Tanaka *et al* (2002)
Δ*hapB/hapB*^{c}	ΔB-HapEegfp-pALB	*pyrG89*; *pabaA1*; *fwA1*; *hapB*Δ::*argB*; pHapE-GFP; pAL4H6HapB (*alcA*p-*hapB*); ArgB$^+$; PyrG$^+$	Steidl *et al* (2004)
Δ*sreA*/Δ*hapB*/*hapB*^{c}		*pyrG89*; *pabaA1*; *biA*; *wA3*; *argB2; sreA*Δ::*argB; hapB*Δ::*argB*; pHapE-GFP; PyrG$^+$; pAL4H6HapB (*alcA*p-*hapB*)	This study
Δ*hapX*/Δ*hapB*		*pyrG89*; y*A*; *argB2*; *pyroA4*; *hapX*Δ::*argB*; *hapB*Δ::*argB*; ArgB$^+$	This study
hapX^R		*pyrG89*; *biA*; *wA3*; *argB2*; *pyroA4*; *hapX*Δ::*argB*; ArgB$^+$; pCAME703-AoHapX-full; PyrG$^+$; pSK275 (PtrA$^+$)	This study
BiFC analysis			
AXB4A2		*pyrG89*, *pabaA1*; *argB2; fwA1*; *bga0*; *argB2*::pAXB4A (*acvA*p-*uidA*; *ipnA*p-*lacZ*); ArgB$^+$	Weidner *et al* (1998)
yXB	*yHapX-HapB*	*pyrG89*, *pabaA1*; *argB2; fwA1*; *bga0*; *argB2*::pAXB4A (*acvA*p-*uidA*, *ipnA*p-*lacZ*); ArgB$^+$; pHapX-YC-pyr4; PyrG$^+$; pHapB-YN	This study
*yXB*Δ*C*	*yHapX-HapB-*Δ*C*	*pyrG89*; *pabaA1*; *riboB*; *hapC*Δ::*riboB*; RiboB$^+$; pHapX-YC-pyr4; PyrG$^+$; pHapB-YN	This study
yXBC^C	*yHapX-HapB-HapC*^{C}	*pyrG89*; *pabaA1*; *riboB*; *hapC*Δ::*riboB*; RiboB$^+$; *pyr-4*::pHapX-YC-pyr4; PyrG$^+$; pHapB-YN*; hapC*::pAlcA-HapC; HapC$^+$; *pabaA1*::PabaAnid; PabaA$^+$	This study
hapE truncation mutants			
hapE-full		*pyrG89*; *biA*; *wA3*; *argB2*; *pyroA4*; *pabaA1*; *hapE*Δ::*argB*; pTG-Taa; PyrG$^+$; ArgB$^+$; pCAME3M-*AohapE-Full*	Tanoue *et al* (2006)
*hapE-*Δ*C*		*pyrG89*; *biA*; *wA3*; *argB2*; *pyroA4*; *pabaA1*; *hapE*Δ::*argB*; pTG-Taa; PyrG$^+$; ArgB$^+$; pCAME3M-*AohapE-*Δ*C*	Tanoue *et al* (2006)
*hapE-*Δ*N*		*pyrG89*; *biA*; *wA3*; *argB2*; *pyroA4*; *pabaA1*; *hapE*Δ::*argB*; pTG-Taa; PyrG$^+$; ArgB$^+$; pCAME3M-*AohapE-*Δ*N*	Tanoue *et al* (2006)
*hapE-*Δ*N*Δ*C*		*pyrG89*; *biA*; *wA3*; *argB2*; *pyroA4*; *pabaA1*; *hapE*Δ::*argB*; pTG-Taa; PyrG$^+$; ArgB$^+$; pCAME3M-*AohapE-*Δ*N*Δ*C*	Tanoue *et al* (2006)
*hapE-*Δ*N*Δ*A*		*pyrG89*; *biA*; *wA3*; *argB2*; *pyroA4*; *pabaA1*; *hapE*Δ::*argB*; pTG-Taa; PyrG$^+$; ArgB$^+$; pCAME3M-*AohapE-*Δ*N*Δ*A*	Tanoue *et al* (2006)
*hapE-*Δ*A*		*pyrG89*; *biA*; *wA3*; *argB2*; *pyroA4*; *pabaA1*; *hapE*Δ::*argB*; pTG-Taa; PyrG$^+$; ArgB$^+$; pCAME3M-*AohapE-*Δ*A*	Tanoue *et al* (2006)

proteins were produced by auto-induction in *E. coli* Rosetta 2 (DE3) cells grown on Overnight Express Instant TB Medium (Novagen), and were subsequently purified to homogeneity, as described in detail in the Supplementary data. The MBP domain was removed from HapC by TEV protease cleavage.

SPR analysis

Real-time analysis was performed on a Biacore 2000 system at 25°C. Data were processed with the BIAevaluation software version 4.1 (Biacore). The running buffer used for DNA immobilization and the SPR analysis was 10 mM HEPES pH 7.4, 0.15 M NaCl, 1 mM DTT, 0.005% (v/v) surfactant P20. Refractive index errors due to bulk solvent effects were corrected by subtracting responses from the non-coated flow cell 1. Sample injection and dissociation time was set to 2.5 min at a flow rate of 30 µl/min.

DNA duplexes containing the CCAAT boxes from the *sreA* (−1257 to −1208) and *lysF* (−200 to −151) promoter regions were generated on an SA sensor chip on flow cells 2 and 3 by injection of 5′-biotinylated 50-bp oligonucleotides B-SREAC1i and B-LYSFC1i (5 nM), at a flow rate of 10 µl/min until 20 RU had been bound. This was followed by injection of oligonucleotides SREAC1 and LYSFC1 (1 µM) until formation of a total of 40 RU DNA duplexes. The CBCs were preformed from the single HapC, HapE (or HapE-ΔNΔA) and HapB proteins by mixing 0.1 mM solutions of each subunit. Samples for SPR analysis were generated by 500-fold dilution of this stock solution in running buffer, followed by serial two-fold dilution.

To avoid possible oxidation reactions caused by DTT-mediated reduction of Fe^{3+} in HEPES buffer (Spear and Aust, 1998), the running buffer for analyses of CBC/HapX interaction in the presence of metal salts contained 10 mM phosphate buffer pH 7.4, 2.7 mM KCl, 137 mM NaCl, 1 mM DTT and 0.005% (v/v) surfactant P20. For metal treatment of HapX, freshly prepared stock solutions of $FeCl_3$, $(NH_4)_2Fe(SO_4)_2$ or $CuCl_2$ were used.

Regeneration of sensor chips was achieved by treatment with the respective running buffer containing additionally 0.5 M NaCl and 0.01% (w/v) SDS for 1 min. Dissociation constants were calculated from the concentration-dependent steady-state binding of the CBCs, using the 1:1 steady-state affinity model.

BiFC analysis

The *hapB* gene was amplified by PCR using primers HapB 5′NcoI and HapB 3′NotI, which also inserted *Nco*I and *Not*I sites at the 5′ and 3′ ends, respectively. The *Nco*I/*Not*I-digested PCR product was inserted into plasmid pEYFPN (Hoff and Kück, 2005), yielding plasmid pYN-HapB, which encodes a C-terminal fusion of HapB with the N-terminal split fragment of eYFP. The *hapX* ORF was amplified by PCR using primers HapX 5′NcoI and HapX 3′NotI, using plasmid pCR2.1-HapX as the template. The *Nco*I/*Not*I-digested PCR product was inserted into plasmid pEYFPC to yield plasmid pYC-HapX, which encodes a C-terminal fusion of HapX with the C-terminal split fragment of eYFP.

Co-transformation of pYC-HapX and pYN-HapB was carried out in both the wild-type strain AXB4A2 and the Δ*hapC* strain. The resulting strains were designated *yXB* and y*XB*Δ*C*, respectively. Strain *yXBC*^{C} was generated by ectopical integration of plasmid pAlcA-HapC, which contains *hapC* under the control of the *alcA* promoter, into strain *yXB*Δ*C*. Plasmid pAlcA-HapC was generated by integration of the *hapC*-containing *Bam*HI/*Xba*I fragment from plasmid pHapC-Topo in plasmid pAL4 (Steidl *et al*, 2001).

Supplementary data
Supplementary data are available at *The EMBO Journal* Online (http://www.embojournal.org).

Acknowledgements

We thank Peter Mayser for helpful discussions and Petra Loitzl for technical assistance in the PpIX determination. Olaf Scheibner is greatfully acknowledged for identification of proteins using mass spectrometry. We thank Birgit Hoff and Ulrich Kück for the gift of BiFC plasmid pEYFPN and pEYFPC, as well as Gary Sawers und Kenton E Barnes for advice regarding the manuscript. This work was supported by Austrian Science Foundation grants FWF P-15959-B11 and FWF P-18606-B11 (HH) and FWF P-19764 (ERW), the Deutsche Forschungsgemeinschaft Priority Program 1152 (AAB), and the Grant-in-Aid for Scientific Research from the Japan Society for the Promotion of Science 16580057 (MK).

References

Becker DM, Fikes JD, Guarente L (1991) A cDNA encoding a human CCAAT-binding protein cloned by functional complementation in yeast. *Proc Natl Acad Sci USA* **88:** 1968–1972

Bonkovsky HL, Wood SG, Howell SK, Sinclair PR, Lincoln B, Healey JF, Sinclair JF (1986) High-performance liquid chromatographic separation and quantitation of tetrapyrroles from biological materials. *Anal Biochem* **155:** 56–64

Bourgarel D, Nguyen CC, Bolotin-Fukuhara M (1999) HAP4, the glucose-repressed regulated subunit of the HAP transcriptional complex involved in the fermentation-respiration shift, has a functional homologue in the respiratory yeast *Kluyveromyces lactis*. *Mol Microbiol* **31:** 1205–1215

Bradshaw RE, Dixon SW, Raitt DC, Pillar TM (1993) Isolation and nucleotide sequence of the 5-aminolevulinate synthase gene from *Aspergillus nidulans*. *Curr Genet* **23:** 501–507

Brakhage AA, Andrianopoulos A, Kato M, Steidl S, Davis MA, Tsukagoshi N, Hynes MJ (1999) HAP-like CCAAT-binding complexes in filamentous fungi: implications for biotechnology. *Fungal Genet Biol* **27:** 243–252

Bucher P (1990) Weight matrix descriptions of four eukaryotic RNA polymerase II promoter elements derived from 502 unrelated promoter sequences. *J Mol Biol* **212:** 563–578

Edwards D, Murray JA, Smith AG (1998) Multiple genes encoding the conserved CCAAT-box transcription factor complex are expressed in *Arabidopsis*. *Plant Physiol* **117:** 1015–1022

Eisendle M, Oberegger H, Zadra I, Haas H (2003) The siderophore system is essential for viability of *Aspergillus nidulans*: functional analysis of two genes encoding l-ornithine *N* 5-monooxygenase (sidA) and a non-ribosomal peptide synthetase (sidC). *Mol Microbiol* **49:** 359–375

Eisendle M, Schrettl M, Kragl C, Muller D, Illmer P, Haas H (2006) The intracellular siderophore ferricrocin is involved in iron storage, oxidative-stress resistance, germination, and sexual development in *Aspergillus nidulans*. *Eukaryot Cell* **5:** 1596–1603

Goda H, Nagase T, Tanoue S, Sugiyama J, Steidl S, Tuncher A, Kobayashi T, Tsukagoshi N, Brakhage AA, Kato M (2005) Nuclear translocation of the heterotrimeric CCAAT binding factor of *Aspergillus oryzae* is dependent on two redundant localising signals in a single subunit. *Arch Microbiol* **184:** 93–100

Haas H (2003) Molecular genetics of fungal siderophore biosynthesis and uptake: the role of siderophores in iron uptake and storage. *Appl Microbiol Biotechnol* **62:** 316–330

Haas H, Schoeser M, Lesuisse E, Ernst JF, Parson W, Abt B, Winkelmann G, Oberegger H (2003) Characterization of the *Aspergillus nidulans* transporters for the siderophores enterobactin and triacetylfusarinine C. *Biochem J* **371:** 505–513

Haas H, Zadra I, Stoffler G, Angermayr K (1999) The *Aspergillus nidulans* GATA factor SREA is involved in regulation of siderophore biosynthesis and control of iron uptake. *J Biol Chem* **274:** 4613–4619

Halliwell B, Gutteridge JM (1984) Oxygen toxicity, oxygen radicals, transition metals and disease. *Biochem J* **219:** 1–14

Harrison KA, Marzluf GA (2002) Characterization of DNA binding and the cysteine rich region of SRE, a GATA factor in *Neurospora crassa* involved in siderophore synthesis. *Biochemistry* **41:** 15288–15295

Hink MA, Bisselin T, Visser AJ (2002) Imaging protein–protein interactions in living cells. *Plant Mol Biol* **50:** 871–883

Hoff B, Kück U (2005) Use of bimolecular fluorescence complementation to demonstrate transcription factor interaction in nuclei of living cells from the filamentous fungus *Acremonium chrysogenum*. *Curr Genet* **47:** 132–138

Hooft van Huijsduijnen R, Li XY, Black D, Matthes H, Benoist C, Mathis D (1990) Co-evolution from yeast to mouse: cDNA cloning of the two NF-Y (CP-1/CBF) subunits. *EMBO J* **9:** 3119–3127

Hu CD, Kerppola TK (2003) Simultaneous visualiation of multiple protein interaction in living cells using multicolor fluorescence complementation analysis. *Nat Biotechnol* **21:** 539–545

Johnson DC, Cano KE, Kroger EC, McNabb DS (2005) Novel regulatory function for the CCAAT-binding factor in *Candida albicans*. *Eukaryot Cell* **4:** 1662–1676

Kato M (2005) An overview of the CCAAT-box binding factor in filamentous fungi: assembly, nuclear translocation, and transcriptional enhancement. *Biosci Biotechnol Biochem* **69:** 663–672

Keng T, Guarente L (1987) Constitutive expression of the yeast HEM1 gene is actually a composite of activation and repression. *Proc Natl Acad Sci USA* **84:** 9113–9117

Kniemeyer O, Lessing F, Scheibner O, Hertweck C, Brakhage AA (2006) Optimisation of a 2-D gel electrophoresis protocol for the human-pathogenic fungus *Aspergillus fumigatus*. *Curr Genet* **49:** 178–189

Lan CY, Rodarte G, Murillo LA, Jones T, Davis RW, Dungan J, Newport G, Agabian N (2004) Regulatory networks affected by iron availability in *Candida albicans*. *Mol Microbiol* **53:** 1451–1469

Li Q, Herrler M, Landsberger N, Kaludov N, Ogryzko VV, Nakatani Y, Wolffe AP (1998) *Xenopus* NF-Y pre-sets chromatin to potentiate p300 and acetylation-responsive transcription from the *Xenopus* hsp70 promoter *in vivo*. *EMBO J* **17:** 6300–6315

Littlejohn TG, Hynes MJ (1992) Analysis of the site of action of the amdR product for regulation of the amdS gene of *Aspergillus nidulans*. *Mol Gen Genet* **235:** 81–88

Litzka O, Then Bergh K, Brakhage AA (1996) The *Aspergillus nidulans* penicillin-biosynthesis gene aat (penDE) is controlled by a CCAAT-containing DNA element. *Eur J Biochem* **238:** 675–682

Liu Z, Butow RA (1999) A transcriptional switch in the expression of yeast tricarboxylic acid cycle genes in response to a reduction or loss of respiratory function. *Mol Cell Biol* **19:** 6720–6728

Maity SN, Vuorio T, de Crombrugghe B (1990) The B subunit of a rat heteromeric CCAAT-binding transcription factor shows a striking sequence identity with the yeast Hap2 transcription factor. *Proc Natl Acad Sci USA* **87:** 5378–5382

Mantovani R (1998) A survey of 178 NF-Y binding CCAAT boxes. *Nucleic Acids Res* **26:** 1135–1143

McNabb DS, Pinto I (2005) Assembly of the Hap2p/Hap3p/Hap4p/Hap5p–DNA complex in *Saccharomyces cerevisiae*. *Eukaryot Cell* **4:** 1829–1839

McNabb DS, Tseng KA, Guarente L (1997) The *Saccharomyces cerevisiae* Hap5p homolog from fission yeast reveals two conserved domains that are essential for assembly of heterotetrameric CCAAT-binding factor. *Mol Cell Biol* **17:** 7008–7018

McNabb DS, Xing Y, Guarente L (1995) Cloning of yeast HAP5: a novel subunit of a heterotrimeric complex required for CCAAT binding. *Genes Dev* **9:** 47–58

Mercier A, Pelletier B, Labbe S (2006) A transcription factor cascade involving Fep1 and the CCAAT-binding factor Php4 regulates gene expression in response to iron deficiency in the fission yeast *Schizosaccharomyces pombe*. *Eukaryot Cell* **5:** 1866–1881

Mulder W, Scholten IH, de Boer RW, Grivell LA (1994) Sequence of the HAP3 transcription factor of *Kluyveromyces lactis* predicts the presence of a novel 4-cysteine zinc-finger motif. *Mol Gen Genet* **245:** 96–106

Oberegger H, Schoeser M, Zadra I, Abt B, Haas H (2001) SREA is involved in regulation of siderophore biosynthesis, utilization and uptake in *Aspergillus nidulans*. *Mol Microbiol* **41:** 1077–1089

Oberegger H, Schoeser M, Zadra I, Schrettl M, Parson W, Haas H (2002a) Regulation of freA, acoA, lysF, and cycA expression by iron availability in *Aspergillus nidulans*. *Appl Environ Microbiol* **68:** 5769–5772

Oberegger H, Zadra I, Schoeser M, Abt B, Parson W, Haas H (2002b) Identification of members of the *Aspergillus nidulans* SREA regulon: genes involved in siderophore biosynthesis and utilization. *Biochem Soc Trans* **30:** 781–783

Oide S, Moeder W, Haas H, Krasnoff S, Gibson D, Yoshioka K, Turgeon BG (2006) NPS6, encoding a non-ribosomal peptide synthetase involved in siderophore-mediated iron metabolism, is a conserved virulence determinant of plant pathogenic ascomycetes. *Plant Cell* **18:** 2836–2853

Pelletier B, Trott A, Morano KA, Labbe S (2005) Functional characterization of the iron-regulatory transcription factor Fep1 from *Schizosaccharomyces pombe*. *J Biol Chem* **280:** 25146–25161

Pinkham JL, Guarente L (1985) Cloning and molecular analysis of the HAP2 locus: a global regulator of respiratory genes in *Saccharomyces cerevisiae*. *Mol Cell Biol* **5:** 3410–3416

Pinkham JL, Olesen JT, Guarente LP (1987) Sequence and nuclear localization of the *Saccharomyces cerevisiae* HAP2 protein, a transcriptional activator. *Mol Cell Biol* **7:** 578–585

Pontecorvo G, Roper JA, Hemmons LM, Macdonald KD, Bufton AW (1953) The genetics of *Aspergillus nidulans*. *Adv Genet* **5:** 141–238

Puig S, Askeland E, Thiele DJ (2005) Coordinated remodeling of cellular metabolism during iron deficiency through targeted mRNA degradation. *Cell* **120:** 99–110

Schrettl M, Bignell E, Kragl C, Joechl C, Rogers T, Arst Jr HN, Haynes K, Haas H (2004) Siderophore biosynthesis but not reductive iron assimilation is essential for *Aspergillus fumigatus* virulence. *J Exp Med* **200:** 1213–1219

Spear N, Aust D (1998) The effects of different buffers on the oxidation of DNA by thiols and ferric ion. *J Biochem Mol Toxicol* **12:** 125–132

Steidl S, Hynes MJ, Brakhage AA (2001) The *Aspergillus nidulans* multimeric CCAAT binding complex AnCF is negatively autoregulated via its hapB subunit gene. *J Mol Biol* **306:** 643–653

Steidl S, Papagiannopoulos P, Litzka O, Andrianopoulos A, Davis MA, Brakhage AA, Hynes MJ (1999) AnCF, the CCAAT binding complex of *Aspergillus nidulans*, contains products of the hapB, hapC, and hapE genes and is required for activation by the pathway-specific regulatory gene amdR. *Mol Cell Biol* **19:** 99–106

Steidl S, Tuncher A, Goda H, Guder C, Papadopoulou N, Kobayashi T, Tsukagoshi N, Kato M, Brakhage AA (2004) A single subunit of a heterotrimeric CCAAT-binding complex carries a nuclear localization signal: piggy back transport of the pre-assembled complex to the nucleus. *J Mol Biol* **342:** 515–524

Sybirna K, Guiard B, Li YF, Bao WG, Bolotin-Fukuhara M, Delahodde A (2005) A new *Hansenula polymorpha* HAP4 homologue which contains only the N-terminal conserved domain of the protein is fully functional in *Saccharomyces cerevisiae*. *Curr Genet* **47:** 172–181

Tanaka A, Kato M, Nagase T, Kobayashi T, Tsukagoshi N (2002) Isolation of genes encoding novel transcription factors which interact with the Hap complex from *Aspergillus* species. *Biochim Biophys Acta* **1576:** 176–182

Tanoue S, Kamei K, Goda H, Tanaka A, Kobayashi T, Tsukagoshi N, Kato M (2006) The region in a subunit of the *Aspergillus* CCAAT-binding protein similar to the HAP4p-recruiting domain of *Saccharomyces cerevisiae* Hap5p is not essential for transcriptional enhancement. *Biosci Biotechnol Biochem* **70:** 782–787

Then Bergh KT, Litzka O, Brakhage AA (1996) Identification of a major *cis*-acting DNA element controlling the bidirectionally transcribed penicillin biosynthesis genes acvA (pcbAB) and ipnA (pcbC) of *Aspergillus nidulans*. *J Bacteriol* **178:** 3908–3916

Tuncher A, Sprote P, Gehrke A, Brakhage AA (2005) The CCAAT-binding complex of eukaryotes: evolution of a second NLS in the HapB subunit of the filamentous fungus *Aspergillus nidulans* despite functional conservation at the molecular level between yeast, *A. nidulans* and human. *J Mol Biol* **352:** 517–533

Weidner G, d'Enfert C, Koch A, Mol PC, Brakhage AA (1998) Development of a homologous transformation system for the human pathogenic fungus *Aspergillus fumigatus* based on the pyrG gene encoding orotidine 5′-monophosphate decarboxylase. *Curr Genet* **33:** 378–385

Weidner G, Steidl S, Brakhage AA (2001) The *Aspergillus nidulans* homoaconitase gene lysF is negatively regulated by the multimeric CCAAT-binding complex AnCF and positively regulated by GATA sites. *Arch Microbiol* **175:** 122–132

